

# Non-iterative One-step Solution for Point Set Registration Problem on Pose Estimation without Correspondence

Yijun Yuan<sup>1</sup>, Dorit Borrmann<sup>2</sup>, Andreas Nüchter<sup>2</sup> and Sören Schwertfeger<sup>1</sup>

**Abstract**—In this work, we propose to directly find the one-step solution for the point set registration problem without correspondences. Inspired by the Kernel Correlation method, we consider the full connected objective function between two point sets, thus avoiding the computation of correspondences. By utilizing least square minimization the transformed objective function is directly solved with existing well-known closed-form solutions, e.g., singular value decomposition, that is usually used for given correspondences. However, using equal weights of costs for each connection will degenerate the solution due to the large influence of distant pairs. Thus, we additionally set a scale on each term to avoid the high cost on non-important pairs. As in feature-based registration methods, the similarity between descriptors of points determines the scaling weight. Given the weights we yield a one step solution. As the runtime is in  $\mathcal{O}(n^2)$ , we also propose a variant with keypoints that strongly reduce the cost. The experiments show, that our proposed method gives a one-step solution without an initial guess. Our method exhibits competitive outliers robustness, accuracy compared with various methods. And it is more stable to large rotation. In addition, though feature based algorithms are more sensitive to noise, Our method still provide better result compared with the feature match initialized ICP.

## I. INTRODUCTION

The point set registration problem has been explored for several decades. Various techniques have been invented, focussing on both efficiency and accuracy. As discussed in [1], it is extremely hard to find the optimal transformation  $\mathbf{T}$  and correspondence matrix  $\mathbf{P}$  simultaneously. The problem has been addressed in [1] by alternating the optimization of  $\mathbf{T}$  and  $\mathbf{P}$ .

In recent decades, a multitude of algorithms have been proposed on 3D registration. They are divided into rigid and non-rigid algorithms [2] and work either iteratively to solve for the transformation matrix with repeatedly matched points [3], [4], [5], [6], [7] or treat the problem as an optimization program that emit the necessity of computing correspondence [8], [9], [10]. With the high capability of regression methods for Deep Neural Networks, there are some attempts to directly solve the transformation by deep neural networks. Researchers start to seek for approaches that directly predict the transformation [11]. However, those trained model highly relies on its learning data that make it both highly costly and not reliable to cases that are not covered by the space of training data.

<sup>1</sup>Both authors are with the School of Information Science and Technology, ShanghaiTech University, China. [yuanwj, soerensch]@shanghaitech.edu.cn

<sup>2</sup>Both authors are with the Department of Informatics VII Robotics and Telematics, Julius-Maximilians-University Würzburg, Germany. [dorit.borrmann, andreas.nuechter]@uni-wuerzburg.de

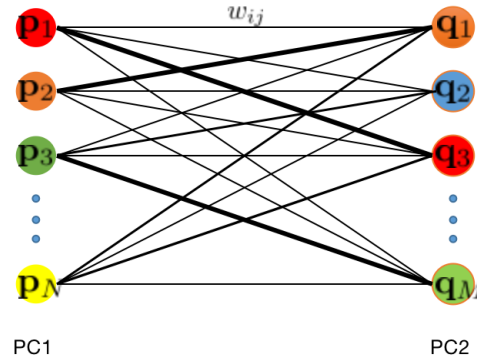


Fig. 1: Full connection between two point sets. Each edge is a weighted Euclidean squared distance term in our object function, given a proper  $w_{i,j}$  to scale the cost term of the pair  $(i, j)$ . The thickness of the lines reflect the similarity (weight) of pairs.

This paper gives a direct solution to the point cloud registration problem without the need of a trained model. There are two problems to address: Correspondence computation and optimization of the objective function. Kernel correlation (KC) [8] is one of the most common registration method that solves the problem without known correspondences by minimizing the full connection cost between two point sets. It is generally in form  $-\mathcal{K}(\mathbf{X}, \mathbf{Y})$  with  $\mathcal{K}$  the kernel. Inspired by the distribution distance, we consider the full connection loss as a good way to omit the correspondence computation.

Aiming at a one-step solution, we first review closed-form results. Given correspondences, there are four known possibilities [12], [13], [14], [15]. The singular value decomposition (SVD) is widely used for computing the optimal rotation  $\mathbf{R}$  and afterwards the optimal translation  $\mathbf{t}$  [15]. Our full connection function builds on this least square solution.

But if each cost term has equivalent effect to object function, the method will fail. In the KC method, the cost term between very distant points only has a tiny impact due to its kernel function. However, in the least square case, large distances will dominate the system and thus do not perform well. Therefore, we properly weight each cost term to suppress the influence of distant point pairs. The weights consider the similarity between two points. Fig. 1 illustrates the full connection, where weights are set according to a similarity measure.

In the following, we first formulate the problem and show some related solutions. Then our method is detailed in

Section II. After that, in Section III we show the experiments for sensitivity to noise, robustness to outlier, and accuracy.

## II. RELATED WORK

The Iterative Closest Point (ICP) algorithm is the most famous registration method. It has been widely applied to various representations of 3D shapes [4] and is able to align a set of range images into a 3D model [5]. The generalized-ICP [6] even puts point-to-point ICP and point-to-plane ICP into one probabilistic framework. ICP consists of two steps, correspondence search and solving for the optimal transformation.

To speed up the search process, point clouds often are stored in  $k$ -d trees. To make it faster, Marden and Guivant [3] propose to use grid data structure to provide a constant time approximate nearest neighbor search. To achieve better quality for matching, especially of very large point clouds, feature based methods are used. Fast Point Feature Histograms (FPFH) are used to analyze the local geometry around a 3D point and provide a basis for the fast computation of a descriptor [7].

Given known correspondences, the transformation can be computed. Walker et al. use dual number quaternions and formulate it as an optimization problem [12]. With a matrix of sum of products of corresponding point coordinates, Horn computes the optimal rotation from the eigenvector associated to the largest positive eigenvalue [13]. This eigenvector is a unit quaternion representing the rotation.

However, the least square form using a matrix representation of rotation is more common. The problem is formulated as follows: Assume we have two point clouds  $\mathbf{P}$  and  $\mathbf{Q}$  with  $\mathbf{p}_i \in \mathbf{P}|_{i \in \{1, \dots, N\}}$  and  $\mathbf{q}_j \in \mathbf{Q}|_{j \in \{1, \dots, M\}}$ . Since we have 3D point clouds,  $\mathbf{p}_i, \mathbf{q}_j \in \mathbb{R}^3$ . Then the optimization task is

$$\min_{\mathbf{R}, \mathbf{t}} \sum_{(i,j) \in \mathcal{C}} \|\mathbf{R}\mathbf{p}_i + \mathbf{t} - \mathbf{q}_j\|^2 \quad (1)$$

where  $\mathbf{R}$ ,  $\mathbf{t}$  are the rotation matrix and translation vector to transform  $\mathbf{P}$  into the coordinate system of  $\mathbf{Q}$ .  $\mathcal{C}$  is the set of correspondences.

With a more widely used orthogonal matrix representation for the rotation, Horn et al. [14] formulate a least square problem and propose a solution using a 3-by-3 matrix. Also relying on a matrix representation, Arun et al. [15] resort to the SVD to solve for the rotation as a multiplication of the two resulting orthonormal matrices.

However, in ICP and related methods, the correspondences have to be re-computed each iteration. To avoid this, the KC method [8] uses an objective function that fully connects the point clouds:

$$\min_{\mathbf{R}, \mathbf{t}} \sum_{i=1}^N \sum_{j=1}^M e^{-\frac{\|\mathbf{R}\mathbf{p}_i + \mathbf{t} - \mathbf{q}_j\|^2}{2\sigma^2}} \quad (2)$$

if Gaussian distances are chosen. In each term of the summation, a robust function, the Gaussian distance, has been utilized. Similar to Maximum Mean Discrepancy (MMD), KC evaluates the distance between two distributions. Thus

it shows better sensitivity to noise and is more robust than ICP-like methods. Many later publications do not rely on correspondences. Myronenko and Song [9] represent point clouds with Gaussian mixture models and solve the transformation by aligning the model centroids. Zheng et al. [10] build a continuous distance field for a fixed model and align the other point set model to minimize the energy iteratively.

Actually, both Equations (1) and (2) have their benefits. While needing to compute the correspondences, Eq. (1) provides a closed-form solution. The KC loss Eq. (2) omits the necessity of finding the correspondences.

We intend to use both full connection and the least square form. However, just replacing the kernel with the quadratic distance will not work due to the distant pairs that will dominate the loss. As discussed in [8], the gradient of the quadratic function is very sensitive to outliers, so a more robust function, the Gaussian kernel, has been utilized. To avoid the fast increase of the gradient, we use additional weights to rebalance each quadratic term in the full connection. The formula is a summation of square distances for each fully connected point pair. The weight  $w_{i,j}$  in the range  $(0, 1]$  has been assigned for each term.

$$\min_{\mathbf{R}, \mathbf{t}} \sum_{i=1}^N \sum_{j=1}^M w_{i,j} \|\mathbf{R}\mathbf{p}_i + \mathbf{t} - \mathbf{q}_j\|^2 \quad (3)$$

Please note that one problem of Gaussian kernel distances in the KC method is, that  $\sigma$  has to be properly set according to the scale of the data. We use the square distance as it is invariant to scale [16]. However, to have the desired suppression effect, weights cannot be arbitrarily chosen. We will discuss the weight in Section II-B.

### A. Solving the Transformation

For the weighted function (3), there is a full connection with quadratic distance between every point  $\mathbf{p} \in \mathbf{P}$  and  $\mathbf{q} \in \mathbf{Q}$ . Then the problem is to reformulate Eq. (3) with full connection as correspondences. The new point sets  $(\mathcal{X}, \mathcal{Y})$  are of size  $NM$  and each pair is a connection.

The optimal solution is obtained with any algorithm that computes the transformation. Here we choose the SVD detailed in [17].

Following [17],  $\mathcal{X} = \{\mathbf{p}'_1, \dots, \mathbf{p}'_{NM}\}$ ,  $\mathcal{Y} = \{\mathbf{q}'_1, \dots, \mathbf{q}'_{NM}\}$ , the problem is formulated as

$$(\mathbf{R}, \mathbf{t}) = \underset{\mathbf{R} \in SO(d), \mathbf{t} \in \mathbb{R}^d}{\operatorname{argmin}} \sum_{i=1}^{NM} w_i \|(\mathbf{R}\mathbf{p}'_i + \mathbf{t}) - \mathbf{q}'_i\|^2 \quad (4)$$

with known weights  $w_i > 0$ .

We cancel  $\mathbf{t}$  by computing the weighted mean

$$\bar{\mathbf{p}}' = \frac{\sum_{i=1}^{NM} w_i \mathbf{p}'_i}{\sum_{i=1}^{NM} w_i}, \bar{\mathbf{q}}' = \frac{\sum_{i=1}^{NM} w_i \mathbf{q}'_i}{\sum_{i=1}^{NM} w_i} \quad (5)$$

and centering the point clouds

$$\mathbf{x}_i := \mathbf{p}'_i - \bar{\mathbf{p}}', y_i := \mathbf{q}'_i - \bar{\mathbf{q}}'. \quad (6)$$

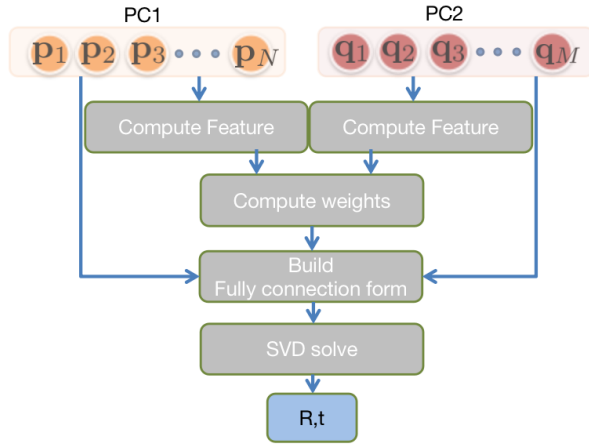


Fig. 2: Pipeline of proposed method.

We can then compute  $\mathbf{R}$

$$\mathbf{R} = \operatorname{argmin}_{\mathbf{R} \in SO(d)} \sum_{i=1}^{NM} w_i \|\mathbf{R}\mathbf{x}_i - \mathbf{y}_i\|^2. \quad (7)$$

Let  $\mathbf{X}$  denote the matrix where  $\mathbf{x}_i$  is the  $i$ -th column. Similarly, we have  $\mathbf{Y}$ . Thus,  $\mathbf{X}, \mathbf{Y} \in \mathbb{R}^{3 \times NM}$ .  $\mathbf{W}$  is a diagonal matrix with  $\mathbf{W}_{i,i} = w_i$ . The SVD solves it where

$$\mathbf{U}\Sigma\mathbf{V}^T = \mathbf{X}\mathbf{W}\mathbf{Y}^T \quad (8)$$

and the optimal rotation is computed by

$$\mathbf{R} = \mathbf{V}\mathbf{U}^T \quad (9)$$

. Finally, the translation is given as

$$\mathbf{t} = \bar{\mathbf{q}}' - \mathbf{R}\bar{\mathbf{p}}'. \quad (10)$$

### B. Weights as a Similarity of Feature

To determine the weights, we use  $f_{\mathcal{X}}(\mathbf{x})$  to denote a function that extracts a feature descriptor of the point  $\mathbf{x}$  from the point cloud  $\mathcal{X}$ . Then the similarity is obtained as

$$w_i = e^{-\frac{1}{\beta} \|f_{\mathcal{X}}(\mathbf{p}'_i) - f_{\mathcal{Y}}(\mathbf{q}'_i)\|^2}. \quad (11)$$

The lower the similarity, the lower the weight of the pairs. Thus, the effect of the term on the objective function will be less. In this way, a pair of points with low similarity contributes only a little, as they have large a feature descriptor distance. The constant  $\beta$  in Eq. (11) scales the feature distance. It depends on the selected feature descriptor. For  $f$  we utilize in our implementation the FPFH [7].

In addition to  $\beta$  and  $f$ , the feature extraction usually depends on the chosen radius. This implies performance changes when using differently scaled data. To make the whole algorithm invariant to scale, FPFH is using the  $k$  nearest neighbor search for the normal and feature extraction. The complete registration pipeline is given in Fig. 2.

### C. Time Complexity

The runtime for the proposed method is dominated by two parts: Computing the weights and solving the SVD. For convenience we assume  $M = N$ . To compute the weight, points descriptors of each point cloud are computed, which takes  $\mathcal{O}(Nk \log N)$ , where  $k$  is the number of neighbors for each point. Then setting up the  $N^2$  weights takes  $\mathcal{O}(N^2)$ . In the SVD, we first compute the centroid and transform the point cloud to center, which takes  $\mathcal{O}(N^2)$ , because we have to consider  $NM$  terms. Since  $\mathbf{W} \in \mathbb{R}^{NM \times NM}$  is a diagonal matrix, the multiplication for  $\mathbf{X}\mathbf{W}\mathbf{Y}^T$  is equivalent to scaling each row  $i$  of  $\mathbf{Y}^T$  with  $\mathbf{W}_{i,i}$ . Thus, to obtain  $\mathbf{X}\mathbf{W}\mathbf{Y}^T$  takes  $\mathcal{O}(N^2)$ . As  $\mathbf{X}\mathbf{W}\mathbf{Y}^T$  is a 3-by-3 matrix, solving the SVD costs only constant time.

Overall, the time complexity of proposed method is with  $\mathcal{O}(N^2)$ .

### D. A Variant: Applying on Point Set of Keypoints

For large point sets, the time complexity of  $\mathcal{O}(N^2)$  becomes infeasible. One possible solution is to extract interest points and to apply the full connection cost to the two sets of keypoints.

Using FPFH the implementation is inexpensive. For each point set with  $N$  points, computing the normals takes  $\mathcal{O}(Nk \log N)$  and keypoint detection takes  $\mathcal{O}(N)$ . Assume  $n$  points are extracted ( $n \ll N$ ), then weight and SVD computation is done on  $n$  points. Overall, we yield  $\max(\mathcal{O}(Nk \log N), \mathcal{O}(n^2))$ .

## III. EXPERIMENTS AND RESULTS

We compare the proposed algorithm with ICP, a feature based (FB) algorithm (feature matching, then ICP), Coherent Point Drift (CPD) and Density Adaptive Point Set Registration (DARE). We call our method Full Connection Form Solution (CF) and CF-keypoint (CFK) (a variant with keypoints) for short.

In our experiments, the small object datasets “bunny”, “dragon”, and “Armadillo” (bun000, dragonStandRight.0 and ArmadilloStand.180) 3D data from the Stanford website<sup>1</sup> have been used to evaluate the sensitivity to noise, the robustness to outliers, and the accuracy of registration, cf. Fig. 4. Then we further apply our algorithm to the large scene datasets LectureHall and Randersacker. The implementation and test code is given in source files that are available in github<sup>2</sup>.

### A. Settings

We first sample the point clouds from the meshes using Meshlab [18]. The CPD is used with the open source C++ implementation referred by original project of [9]. We have set its scale and reflection parameters to false. For DARE we use the python implementation of [19]. Its color label and feature label are disabled. We have implemented the ICP, CF and CFK using the Point Cloud Library (PCL) [20]. FB is

<sup>1</sup><http://graphics.stanford.edu/data/3Dscanrep/>

<sup>2</sup>Added after acceptance

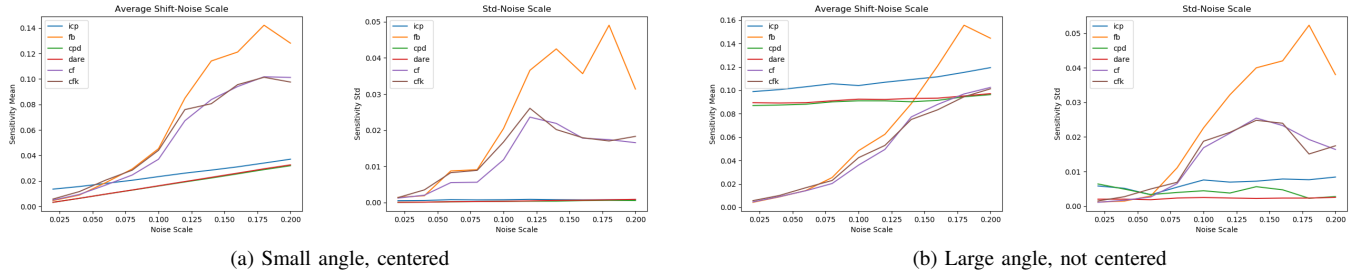


Fig. 3: Sensitivity test. The left two plots show results with small rotation, centered. The right two plots show results with large rotation, not centered. The first and third image refer to mean shift to noise scale. The second and fourth image refer to the standard deviation. Noise scale is the standard deviation for the zero mean norm noise.

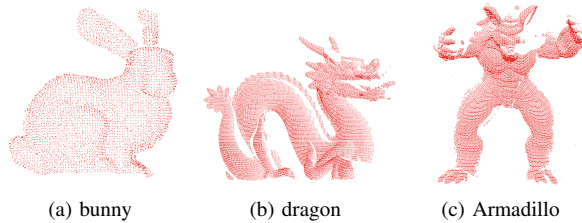


Fig. 4: Three point cloud used for experiments.

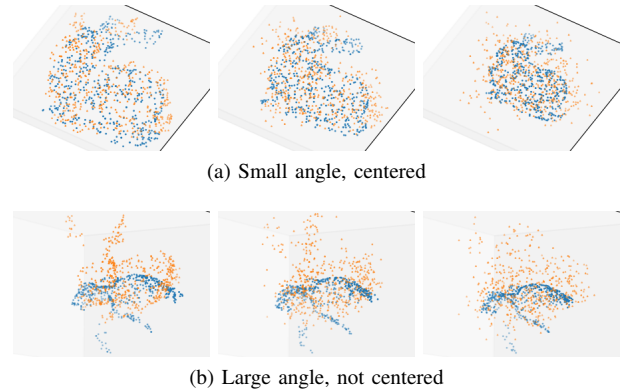


Fig. 5: Noise data. Above: centered small angle, below: large angle. From left to right column is with noise standard derivation 0.02, 0.1 and 0.2.

used with a well implemented feature match initialized ICP<sup>3</sup>.

For the feature based registration (FB), we use FPFH descriptor and RANSAC. The final refinement is done via ICP from PCL. For CF and CFK, we also use FPFH descriptor from PCL. The normal and feature computation in FB, CF and CFK are performed with the same settings, i.e., searching  $k$  neighbors. In our implementation we fixed  $k$  to 150. In addition, the  $\beta$  used in Eq. (11) is fixed to 100.

In our experiments, the registration is done using two point clouds  $PC_a$  and  $PC_b$  that were generated from one original point cloud. Then, we transformed  $PC_b$  to have  $PC'_b$ . So the  $PC_a$  is our PC1 and  $PC'_b$  is our PC2 and our task is to align PC1 to PC2 by solving for the transformation. We apply two transformations to the original point cloud. One is translating the point cloud to make the gravity center the origin and then apply a small rotation angle. The second is to directly rotate a large angle without any translation.

### B. Sensitivity to Noise

PC1 and PC2 are subsampled to 500 points. For the rotated set PC2, we add zero mean Gaussian noise to each point. For evaluation after registration, we compute the average shift between the corresponding points after 30 trials. Following the definition of sensitivity [8], we log the mean average shift to evaluate the performance and the standard deviation is utilized as the metric. The noise scale is within the range  $(0, 0.2]$ . Because the size of the bunny does not exceed

0.3, too large noise will result in dysfunctional feature descriptors. We present the noise data with different noise scale in Fig. 5. The results are given in Fig. 3.

For the centered small rotation, ICP, CPD and DARE achieve better average shifts and less sensitivities to the noise. For the feature based methods, our CF and CFK outperform FB.

However, for the large rotation data, both ICP, CPD and DARE fail to align the point clouds, while the feature based methods CF, CFK, and FB are able to align with good performance. In addition, our CF and CFK achieve better alignments, even with respect to sensitivity, than FB, given increasing noise.

TABLE I: Robustness test: smaller is better.

	Small rotation, centered	Large rotation, not centered
ICP	$0.011 \pm 0.0069$	$0.080 \pm 0.018$
FB	$0.0097 \pm 0.0065$	$0.0084 \pm 0.0049$
CPD	$2.4e - 09 \pm 1.7e - 10$	$0.040 \pm 0.047$
DARE	$0.012 \pm 0.020$	$0.054 \pm 0.034$
CF	$0.0075 \pm 0.0028$	$0.0078 \pm 0.0032$
CFK	$0.0100 \pm 0.0050$	$0.010 \pm 0.0055$

<sup>3</sup><https://github.com/andymiller/FeatureBasedAlignment>

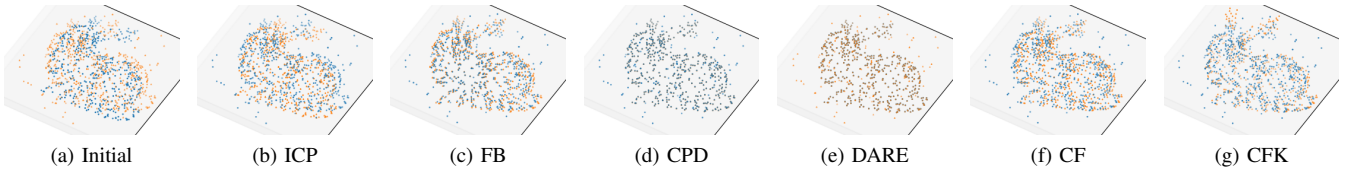


Fig. 6: Robustness test: Example from the small rotation set, centered.

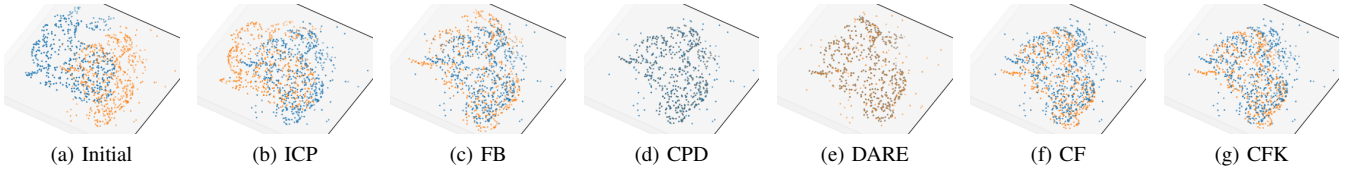


Fig. 7: Robustness test: Medium rotation example from the large rotation set, not centered.

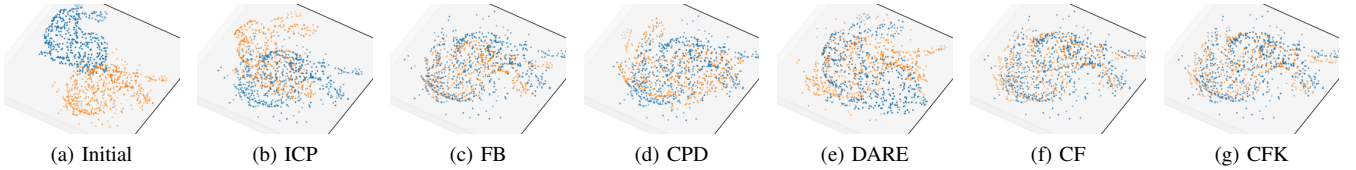


Fig. 8: Robustness test: Large rotation example from the large rotation set, not centered.

### C. Robustness to Outliers

Similarly, we also use 500 randomly selected points from the bunny object and perform small and large rotations. Then 100 random points have been uniformly drawn in a spherical way and added to the rotated point set PC2 (with radius 0.2, around the center of sampled point clouds).

Because the first 500 points in each set are also from the same sampled index, we actually know the correspondence in the non-outlier parts. To quantify the robustness, we compute the average shift as in subsection III-B.

For the centered small rotations, rotation vectors with the value drawn uniformly from  $[-\pi/8, \pi/8]$  have been used. The rotation vector is a concise axis-angle representation, for which both the rotation axis and angle are represented in a 3-vector. The rotation angle is the length of this vector. For the large rotation the vectors are uniformly drawn from  $[-\pi/2, \pi/2]$ .

For both large and small rotations, we test 100 times to record the mean and standard deviation. The quantitative evaluation is given in Table I. Selected visualizations of the alignment are presented in Fig. 6, Fig. 7, and Fig. 8. All experiments have been made using randomly drawn rotation vectors.

CPD achieves extremely precise solutions for small rotations, while feature based methods (FB, CF, CFK) are similar and are better than ICP and DARE. DARE gives the largest error and standard deviation. For the large rotation case, the feature based methods (FB, CF, CFK) perform best and the errors of remaining methods are several times worse and unstable, since they yield large standard deviations. FB has

better results than ICP, which is due to the significance of pose initialization of ICP. Also here, our CF method achieves the best performance.

We select tests with one centered small rotation and two large rotation for demonstration. In Fig. 6 and Fig. 7, CPD and DARE achieve better alignment while it fails in Fig. 8. However, our CF and CFK keep similar results, but are affected by the outliers.

### D. Accuracy

Using the same given transformation applied to the original point sets as in subsection III-C, we achieve rotated models. Then we randomly sample 500 points from both the reference model and the rotated models for testing. To evaluate the accuracy, deviations from the identity matrix [21] are computed:

$$ACC_{\mathbf{R}_{\text{gt}}}(\mathbf{R}_{\text{predicted}}) = \|\mathbf{I} - \mathbf{R}_{\text{predicted}}\mathbf{R}_{\text{gt}}^T\|_F$$

It is a distance measure using the Frobenius norm of a matrix, where  $\mathbf{R}_{\text{gt}}$  is the given rotation and  $\mathbf{R}_{\text{predicted}}$  is the predicted rotation.

Accuracy results are given in Table II. For the centered small rotation case, we observe that CPD also achieves the best score while FB, CF and CFK are on the same level. While for large rotations, CPD become unstable, which results in much larger average rotation distances and its standard deviations. The feature based methods still show similar results in different cases. In addition, our CF is better in both cases comparing to FB and achieves the best performance in the large angle case.

TABLE II: Accuracy test: smaller is better.

	Small rotation, centered			Large rotation, not centered		
	bun	dragon	Armadillo	bun	dragon	Armadillo
ICP	$0.19 \pm 0.12$	$0.19 \pm 0.13$	$0.16 \pm 0.13$	$1.5 \pm 0.70$	$1.50 \pm 0.79$	$1.49 \pm 0.81$
FB	$0.48 \pm 0.61$	$0.39 \pm 0.49$	$0.47 \pm 0.59$	$0.38 \pm 0.44$	$0.30 \pm 0.34$	$0.32 \pm 0.38$
CPD	$0.016 \pm 0.0089$	$0.014 \pm 0.0083$	$0.012 \pm 0.0074$	$1.15 \pm 1.30$	$1.11 \pm 1.19$	$1.13 \pm 1.15$
DARE	$0.020 \pm 0.0095$	$0.016 \pm 0.0090$	$0.017 \pm 0.0082$	$1.31 \pm 1.25$	$1.35 \pm 1.20$	$1.47 \pm 1.16$
<b>CF</b>	$0.16 \pm 0.10$	$0.19 \pm 0.13$	$0.28 \pm 0.36$	$0.18 \pm 0.14$	$0.13 \pm 0.11$	$0.15 \pm 0.12$
CFK	$0.27 \pm 0.29$	$0.26 \pm 0.24$	$0.35 \pm 0.39$	$0.25 \pm 0.23$	$0.22 \pm 0.28$	$0.25 \pm 0.35$

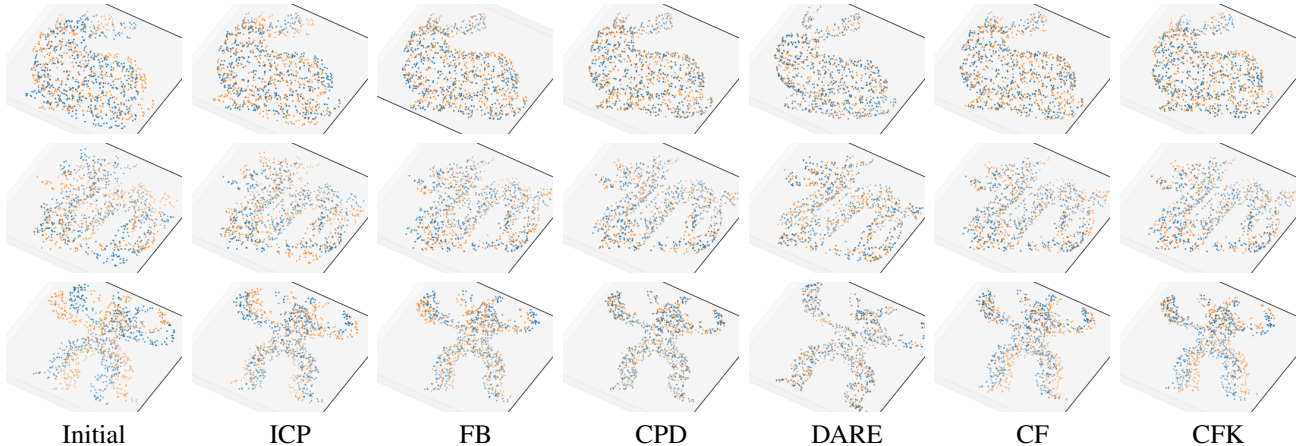


Fig. 9: Accuracy test: Example from the small rotation set, centered.

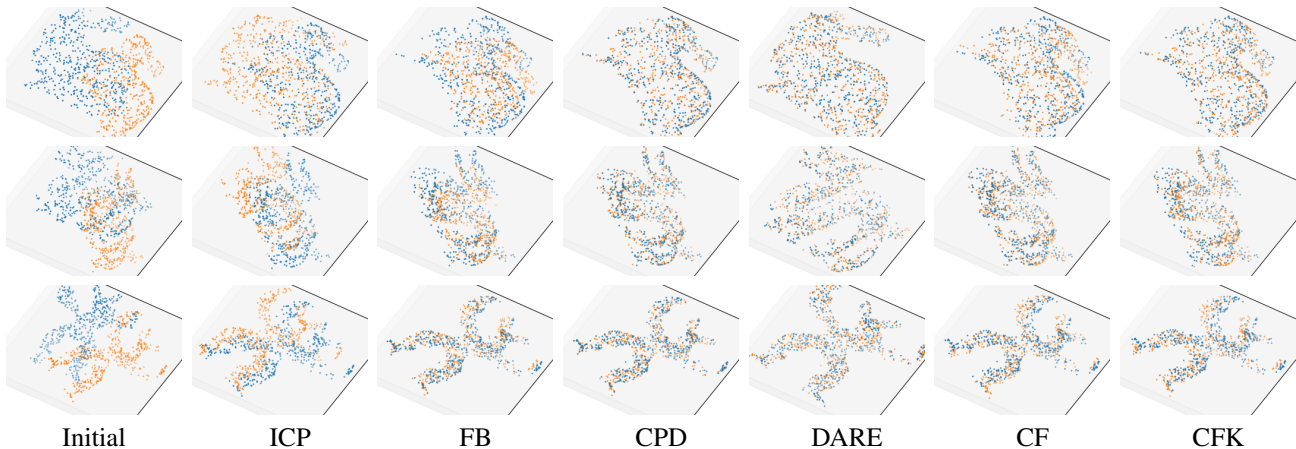


Fig. 10: Accuracy test: Medium rotation example from the large rotation set, not centered.

All of FB, CPD, DARE, CF and CFK perform well. We also present Fig. 9, Fig. 10 and Fig. 11 that correspond with the same rotation vector as Fig. 6, Fig. 7 and Fig. 8. Similarly, CPD and DARE achieve best result in Fig. 9, Fig. 10 and fails in Fig. 11 while the results of the feature based methods (FB, CF, CFK) are close. In addition, our CF and CFK provides better alignment than FB.

#### IV. DISCUSSION

From the experiments, we find the feature based algorithms (FB, CF, CFK) are more sensitive to noise. Though with very small initial rotation, the noise still has impact on

the result. In the outliers test, CPD yields very precise result. The CF algorithm scores second.

However, we also test with large rotation angles and observe that the feature based algorithms are not affected which is observed by its very close results in the curves and tables. While the remaining methods fail or have a large errors comparing to their performance in the centered small angle case.

In the last test, we have removed other effects and take only rotations into consideration. We find that the feature based algorithms are not influenced by the initial angles, while ICP, CPD and DARE are more sensitive to it. It is

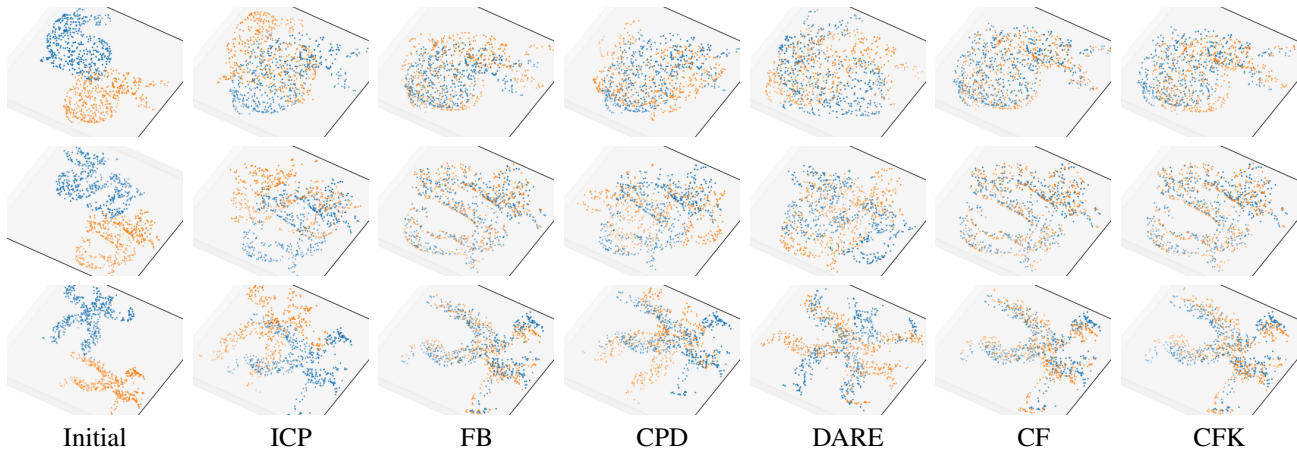


Fig. 11: Accuracy test: Large rotation example from the large rotation set, not centered.

obvious, that in the small angle test, CPD provides extremely good alignments. But the algorithm is not stable to various rotations. So a proper way to use ICP, CPD and DARE related algorithm requires first providing a coarse rotation.

Over all of those tests, the feature-based algorithms, our CF works better than the rest and its variant, CFK achieves very close result.

We also try our method on the Würzburg City dataset<sup>4</sup>. After subsampling, we generate two point sets from the first scan by randomly selecting 30000 points each and rotating one of them with a large rotation. We apply CFK on the data and it well aligns the point cloud as seen in Fig. 12a and Fig. 12b. When trying to align two partially overlapping scans (0 and 1) the method fails as depicted in Fig. 12c.

This leads to the conclusion that the proposed method works well for two point sets from the same distribution. However, it is prone to errors for partially overlapping data. Future work will focus on more distinctive features and weights designed to address this problem. This way the method will be applicable to various kinds of data, especially those with partial overlap.

## V. CONCLUSIONS

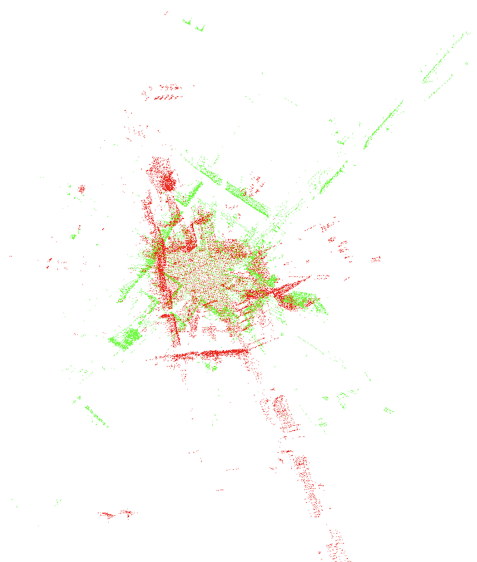
In this paper we have proposed a new solution to the point set registration problem that does not require correspondences. From our survey, this is the first algorithm that directly provides accurate registrations in a non-iterative one-step setup, where the derived formulas have closed-form solution. Future work will focus on investigating different feature descriptors and weights to achieve better robustness for partially overlapping data. The experiments in this paper demonstrate competing performance to various methods in robustness to outliers and accuracy. The feature based algorithms (FB, CF, CFK) are more sensitive to noise compared to the non-feature based methods due to defuncting descriptors. Overall, our CF and CFK provide better performance than FB and with respect to outliers and accuracy it scores competitively compared to all methods.

The non-feature based methods fail or give much worse results while our methods are more stable at large rotations and thus achieve better scores and standard deviations.

## REFERENCES

- [1] H. Li and R. Hartley, "The 3d-3d registration problem revisited," in *2007 IEEE 11th international conference on computer vision*. IEEE, 2007, pp. 1–8.
- [2] B. Bellekens, V. Spruyt, R. Berkvens, and M. Weyn, "A survey of rigid 3d pointcloud registration algorithms," in *AMBIENT 2014: the Fourth International Conference on Ambient Computing, Applications, Services and Technologies, August 24-28, 2014, Rome, Italy*, 2014, pp. 8–13.
- [3] S. Marden and J. Guivant, "Improving the performance of icp for real-time applications using an approximate nearest neighbour search," in *Proceedings of the Australasian Conference on Robotics and Automation, Wellington, New Zealand*, 2012, pp. 3–5.
- [4] P. J. Besl and N. D. McKay, "Method for registration of 3-d shapes," in *Sensor Fusion IV: Control Paradigms and Data Structures*, vol. 1611. International Society for Optics and Photonics, 1992, pp. 586–607.
- [5] S. Fantoni, U. Castellani, and A. Fusiello, "Accurate and automatic alignment of range surfaces," in *2012 Second International Conference on 3D Imaging, Modeling, Processing, Visualization & Transmission*. IEEE, 2012, pp. 73–80.
- [6] A. Segal, D. Haehnel, and S. Thrun, "Generalized-icp," in *Robotics: science and systems*, vol. 2, no. 4, 2009, p. 435.
- [7] R. B. Rusu, N. Blodow, and M. Beetz, "Fast point feature histograms (fpfh) for 3d registration," in *2009 IEEE International Conference on Robotics and Automation*. IEEE, 2009, pp. 3212–3217.
- [8] Y. Tsin and T. Kanade, "A correlation-based approach to robust point set registration," in *European conference on computer vision*. Springer, 2004, pp. 558–569.
- [9] A. Myronenko and X. Song, "Point set registration: Coherent point drift," *IEEE transactions on pattern analysis and machine intelligence*, vol. 32, no. 12, pp. 2262–2275, 2010.
- [10] B. Zheng, R. Ishikawa, T. Oishi, J. Takamatsu, and K. Ikeuchi, "A fast registration method using ip and its application to ultrasound image registration," *IPSJ Transactions on Computer Vision and Applications*, vol. 1, pp. 209–219, 2009.
- [11] S. Miao, Z. J. Wang, and R. Liao, "A cnn regression approach for real-time 2d/3d registration," *IEEE transactions on medical imaging*, vol. 35, no. 5, pp. 1352–1363, 2016.
- [12] M. W. Walker, L. Shao, and R. A. Volz, "Estimating 3-d location parameters using dual number quaternions," *CVGIP: Image Understanding*, vol. 54, pp. 358 – 367, November 1991.
- [13] B. K. P. Horn, "Closed-form solution of absolute orientation using unit quaternions," *Journal of the Optical Society of America A*, vol. 4, no. 4, pp. 629 – 642, April 1987.

<sup>4</sup><http://kos.informatik.uni-osnabrueck.de/3Dscans/>



(a) Align data from same distribution. Initial state.



(b) Align data from same distribution. Aligned.



(c) Align two frames.

Fig. 12: Align the Würzburg city data.

July 1988.

- [15] K. S. Arun, T. S. Huang, and S. D. Blostein, "Least square fitting of two 3-d point sets," *IEEE Transactions on Pattern Analysis and Machine Intelligence*, vol. 9, no. 5, pp. 698 – 700, September 1987.
- [16] F. Fleuret and H. Sahbi, "Scale-invariance of support vector machines based on the triangular kernel," in *3rd International Workshop on Statistical and Computational Theories of Vision*, 2003, pp. 1–13.
- [17] O. Sorkine, "Least-squares rigid motion using svd," *Technical notes*, vol. 120, no. 3, p. 52, 2009.
- [18] P. Cignoni, M. Callieri, M. Corsini, M. Dellepiane, F. Ganovelli, and G. Ranzuglia, "Meshlab: an open-source mesh processing tool." in *Eurographics Italian chapter conference*, vol. 2008, 2008, pp. 129–136.
- [19] F. Järemo Lawin, M. Danelljan, F. Shahbaz Khan, P-E. Forssén, and M. Felsberg, "Density adaptive point set registration," in *Proceedings of the IEEE Conference on Computer Vision and Pattern Recognition*, 2018, pp. 3829–3837.
- [20] R. B. Rusu and S. Cousins, "Point cloud library (pcl)," in *2011 IEEE international conference on robotics and automation*, 2011, pp. 1–4.
- [21] P. M. Larochelle, A. P. Murray, and J. Angeles, "A distance metric for finite sets of rigid-body displacements via the polar decomposition," *Journal of Mechanical Design*, vol. 129, no. 8, pp. 883–886, 2007.

- [14] B. K. P. Horn, H. M. Hilden, and S. Negahdaripour, "Closed-form solution of absolute orientation using orthonormal matrices," *Journal of the Optical Society of America A*, vol. 5, no. 7, pp. 1127 – 1135,